Hindawi
International Journal of Antennas and Propagation
Volume 2019, Article ID 5943956, 13 pages
https://doi.org/10.1155/2019/5943956

Research Article

Classification and Localization of Mixed Sources after Blind Calibration of Unknown Mutual Coupling

Kai Wang,[1] **Ling Wang**,[1] **Jian Xie**,[1] **and Yuexian Wang**[1,2]

[1]*School of Electronics and Information, Northwestern Polytechnical University, Xi'an 710072, China*
[2]*School of Electrical and Electronic Engineering, The University of Adelaide, Adelaide, SA 5005, Australia*

Correspondence should be addressed to Kai Wang; wangk829@sina.com

Received 28 November 2018; Revised 9 March 2019; Accepted 22 April 2019; Published 2 June 2019

Academic Editor: Shiwen Yang

In order to deal with the problem of passive mixed source localization under unknown mutual coupling, the authors propose an effective algorithm. This algorithm provides array blind calibration as well as classification and localization of mixed sources in this paper. In practice, an ideal sensor array without the effects of unknown mutual coupling is rarely satisfied, which degrades the performance of most high-resolution algorithms. Firstly, the directions of arrival of far-field sources and the number of nonzero mutual coupling coefficients are estimated directly through the rank-reduction type method. Then, these estimates are adopted to reconstruct the mutual coupling matrix. In addition, the fourth-order cumulant technique is required to eliminate the Gauss colored noise effects caused by mutual coupling calibration of the raw received data vector. Finally, in an algebraic way, the results of rapid classification and localization of near-field sources are obtained without any spectral search. The proposed algorithm is described in detail, and its behavior is illustrated by numerical examples.

1. Introduction

Passive mixed source localization using array signal processing techniques has received considerable attention over the past decades. For a far-field (FF) source with plane wave front, only the direction of arrival (DOA) parameter is required to be estimated. In the past decades, large numbers of high-resolution algorithms have been proposed to deal with the DOA estimation problem of FF sources, such as estimation of signal parameters via rotational invariance technique (ESPRIT) [1, 2] and multiple signal classification (MUSIC) method [3, 4]. However, all aforementioned algorithms generally work based on the assumption of ideal array. It means that there is no any steering vectors mismatch caused by the unknown mutual coupling [5] or the spherical wave front effect [6] in array.

However, in many interesting applications, some incident sources may locate in the Fresnel Region defined as the near-field (NF) of an array, and these sources are defined as NF sources [7]. For an arbitrary NF source, both DOA and range parameters are required to be estimated since the assumption of plane wave front is no longer valid. Therefore, the traditional algorithms of FF sources' DOA estimation would have inefficient results for NF sources' parameters estimation. Various types of algorithms have been developed in the past decades for the NF sources' localization, such as the reduced rank (RERA) type methods [8–11], the covariance approximation (CA) type algorithms [12, 13], the two-dimensional (2D) MUSIC algorithm [5], and the weighted linear prediction method [14]. Although all the aforementioned algorithms focus on the pure FF or NF sources scenario [15], it is more realistic in many applications where FF and NF sources coexist, such as electronic surveillance, seismic exploration, and speaker localization via microphone arrays. Unfortunately, all the above-mentioned algorithms may fail to deal with the problem of mixed sources classification and localization.

Recently, a large number of algorithms have been developed to manage the mixed sources problem [16–23]. Herein, a fourth-order cumulant (FOC) based MUSIC (Cum4MUSIC) algorithm has been proposed to solve the mixed sources problem by Liang, which has used the property of high order cumulant (HOC) technique to transform the NF sources into FF ones [16]. However, this algorithm may fail to manage

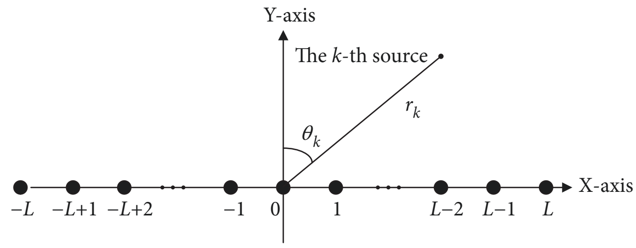

Figure 1: The uniform linear array configuration.

the problem of mixed sources classification because the FOC matrix contains only the FF components. In [17], an oblique projection MUSIC (OPMUSIC) algorithm based on second-order cumulant (SOC) has been presented by Zhi. Although this algorithm has low computational complexity, it has greater loss of array aperture. In order to fully utilize the array aperture to implement the mixed sources classification, a two-stage matrix differencing based MUSIC (TSMUSIC) algorithm has been presented by Liu and it provided a reasonable simulation result [20]. However, the above-mentioned algorithms deal with the problem without mutual coupling compensation.

As well known, the performances of all above-mentioned algorithms obviously degrade without array calibration. In order to deal with the problem, lots of mutual coupling modeling methods and DOA estimation algorithms of FF sources have been presented [24–29]. In [24, 25], various middle subarray methods are presented to estimate DOAs by setting auxiliary sensors, without calibration. However, these methods suffer from a great aperture loss. In [26], a method based on FOC has been presented to deal with the problem of aperture loss. Another popular type of methods against mutual coupling effect is based on the RERA type algorithms [26–30]. These methods take full advantage of array aperture. Thus, they are expected to provide a better estimation performance. However, all the methods in [24–30] must work under the condition of that the accurate number of nonzero elements in the mutual coupling matrix (MCM) has been known. It is the most important structure parameter to reconstruct the MCM.

In this paper, an effective algorithm is presented to deal with the problem of mixed sources classification and localization under unknown mutual coupling. According to the symmetric Toeplitz property of MCM in uniform linear array (ULA), a RERA estimating function is constructed to estimate the FF sources' DOAs and the structure parameter. In this way, it can reduce the multiparameter search into a two-dimensional (2D) search. After the FF sources' DOAs and structure parameter being estimated, the MCM can be reconstructed. Then, the FOC technique is used to eliminate the Gauss colored noise due to mutual coupling calibration of the raw received data vector. Finally, based on array segmentation, we can obtain the results of mixed sources rapid classification and reliable NF sources localization in an algebraic way.

2. Signal Model

Consider K (NF and FF) narrowband and independent signal sources, impinging on a ULA with $2L+1$ omnidirectional sensors, as shown in Figure 1. We assume that there are K_1 NF incident sources in the Fresnel Region and the rest K_2 incident sources are FF sources, where $K_2 = K - K_1$.

Firstly, we model the ideal array received signal vector model without any unknown mutual coupling effect. Without loss of generality, from left to right, the sensors are indexed by $-L, -(L-1), \ldots, L-1, L$ and the centre of array is set to be the phase reference point whose index is zero. The signals received by the l-th sensor can be expressed as

$$x_l(t) = \sum_{k=1}^{K} s_k(t)\, e^{j\tau_{lk}} + n_l(t) \qquad l = -L, -L+1, \ldots, L-1, L \tag{1}$$

where $s_k(t)$ is the k-th narrowband source and $n_l(t)$ is the additive Gaussian white noise. τ_{lk} is the phase shift associated with the k-th source propagation time delay between the 0-th and the l-th sensors. It is straightforward to show that the phase shift between the phase reference point and l-th sensor can be expressed as

$$\tau_{lk} = \frac{2\pi}{\lambda}\left(\sqrt{r_k^2 + (ld)^2 - 2r_k ld \sin\theta_k} - r_k\right) \tag{2}$$

where λ denotes the signal free-space wavelength. $\theta_k \in [-\pi/2, \pi/2]$ is the DOA of the k-th source and $r_k \in [0.62(D^3/\lambda)^{1/2}, +\infty)$ is the range of the k-th source measured from the ULA centre. Herein, $D = 2Ld$ represents the aperture of the array and d is the constant interelement spacing set as $d \le \lambda/8$. According to Taylor series expansion, τ_{lk} can be approximately given as follows [31]:

$$\begin{aligned}
\tau_{lk} &= \alpha_k l + \beta_k l^2 + O\left(l^3\right) \approx \alpha_k l + \beta_k l^2 \\
\alpha_k &= -2\pi \frac{d}{\lambda} \sin\theta_k \\
\beta_k &= \pi \frac{d^2}{\lambda r_k} \cos\theta_k
\end{aligned} \tag{3}$$

Thus, (1) can be approximately expressed as

$$x_l(t) = \sum_{k=1}^{K} s_k(t) e^{j(\alpha_k l + \beta_k l^2)} + n_l(t) \tag{4}$$

As a result, it is obvious that any FF source can be seen as a generalized NF one whose range parameter increases towards the infinite.

According to the discussion in [5], the amplitude of mutual coupling coefficient (MCC) is in inverse proportion to the physical distance between each pair of sensors. In other words, the MCCs between neighbouring sensors with the same adjacent space are almost equal to each other. Besides, the MCC is approximately equal to zero when any two sensors are located enough far from each other. Unfortunately, most of the aforementioned algorithms work without unknown mutual coupling effect elimination, which would lead to fatal performance degradation of these algorithms.

According to the above discussion, the authors firstly model a $(2L+1) \times (2L+1)$ MCM containing $P+1$ $(0 \le P \le L\text{-}1)$ unknown nonzero MCCs. In many papers, those algorithms work under a prior knowledge of the accurate value of P. However, in practice, the parameter P is unknown and it must be effectively estimated in order to reconstruct the correct MCM. We define that $\mathbf{c}(P)$ denotes the $L \times 1$ vector containing $P+1$ unknown nonzero and L-1-P zero MCCs

$$\begin{aligned} \mathbf{c}(P) &= \left[1, c_1, \ldots, c_P, 0, \ldots, 0\right]^T \\ &= \left[1, \mathbf{c}_1{}^T(P), \mathbf{0}_{(L-1-P)\times 1}{}^T\right]^T \end{aligned} \tag{5}$$

where $\mathbf{0}_{(L-1-P)\times 1}$ denotes a $(L\text{-}1\text{-}P)\times 1$ zero vector. Thus, the $(2L+1) \times (2L+1)$ symmetric Toeplitz MCM matrix $\mathbf{C}(P)$ can be modeled as follows:

$$\begin{aligned} \mathbf{C}(P) &= \text{toeplitz}\{\mathbf{c}(P)\} \\ &= \begin{bmatrix} 1 & c_1 & \cdots & c_P & 0 & \cdots & 0 \\ c_1 & 1 & c_1 & \ddots & \ddots & \ddots & \vdots \\ \vdots & c_1 & \ddots & \ddots & \ddots & \ddots & 0 \\ c_P & \ddots & \ddots & \ddots & \ddots & \ddots & c_P \\ 0 & \ddots & \ddots & \ddots & \ddots & c_1 & \vdots \\ \vdots & \ddots & \ddots & \ddots & c_1 & 1 & c_1 \\ 0 & \cdots & 0 & c_P & \vdots & c_1 & 1 \end{bmatrix} \end{aligned} \tag{6}$$

where Toeplitz $\{\mathbf{c}(P)\}$ denotes the $(2L+1)\times(2L+1)$ symmetric Toeplitz matrix constructed by the vector $\mathbf{c}(P)$. It must be noticed that the MCM will be an identity matrix only if $P = 0$, which means there is no mutual coupling effect in the array. However, an ideal array with one-eight wave length interspace without mutual coupling effect is usually unavailable.

Therefore, the received signal vector under the unknown mutual coupling can be expressed in a matrix form

$$\mathbf{X}(t) = \mathbf{C}(P)\mathbf{A}_{\mathrm{N}}\mathbf{S}_{\mathrm{N}}(t) + \mathbf{C}(P)\mathbf{A}_{\mathrm{F}}\mathbf{S}_{\mathrm{F}}(t) + \mathbf{N}(t) \tag{7}$$

where $\mathbf{S}_{\mathrm{N}}(t)$ and $\mathbf{S}_{\mathrm{F}}(t)$ denote the NF signal vector and FF one, respectively,

$$\mathbf{S}_{\mathrm{N}}(t) = \left[s_1(t), \ldots, s_{K_1}(t)\right]^T \tag{8}$$

$$\mathbf{S}_{\mathrm{F}}(t) = \left[s_{1+K_1}(t), \ldots, s_K(t)\right]^T \tag{9}$$

$\mathbf{N}(t)$ signifies a $L \times 1$ dimensional complex noise vector,

$$\mathbf{N}(t) = \left[n_{-L}(t), \ldots, n_L(t)\right]^T \tag{10}$$

And $\mathbf{A}_{\mathrm{N}}$ and $\mathbf{A}_{\mathrm{F}}$ denote the steering vectors of NF and FF sources, respectively, as

$$\mathbf{A}_{\mathrm{N}} = \left[\mathbf{a}(\theta_1, r_1), \ldots, \mathbf{a}\left(\theta_{K_1}, r_{K_1}\right)\right] \tag{11}$$

$$\mathbf{A}_{\mathrm{F}} = \left[\mathbf{a}\left(\theta_{K_1+1}, \infty\right), \ldots, \mathbf{a}(\theta_K, \infty)\right] \tag{12}$$

$$\begin{aligned} \mathbf{a}(\theta_k, r_k) = \Big[& e^{j\{\alpha_k(-L)+\beta_k L^2\}}, e^{j\{\alpha_k(-L+1)+\beta_k(L-1)^2\}}, \ldots, \\ & e^{j\{\alpha_k L+\beta_k L^2\}}\Big]^T \end{aligned} \tag{13}$$

$$\mathbf{a}(\theta_k, \infty) = \left[e^{j\alpha_k(-L)}, e^{j\alpha_k(-L+1)}, \ldots, e^{j\alpha_k L}\right]^T \tag{14}$$

Throughout the paper, the following hypotheses are assumed to hold.

(1) The incoming source signals are statistically independent and zero-mean stationary random process.

(2) The sensor noise is the additive Gaussian White one, which is independent from the source signals.

(3) The number of sources K, K_1, and K_2 are known as prior knowledge, and the number of sensors satisfies $K \le L+1$.

3. Proposed Solution to Localization

The proposed method works in three steps. Firstly, the FF sources' DOAs as well as the accurate value of parameter P are estimated under unknown mutual coupling. And then the MCM is reconstructed based on the estimates in the previous step. Finally, the FOC technique is used to eliminate the noise effect and estimate both DOA and range parameters of NF sources in an algebraic way without spectrum search.

3.1. FF DOA and Parameter P Estimation. According to (7) and the aforementioned assumptions, the received signal covariance matrix can be calculated by

$$\begin{aligned} \mathbf{R} &= E\left\{\mathbf{X}(t)\mathbf{X}^H(t)\right\} \\ &= \mathbf{C}(P)\mathbf{A}_{\mathrm{N}}\sum_{\mathrm{N}}\mathbf{A}_{\mathrm{N}}{}^H\mathbf{C}^H(P) \\ &\quad + \mathbf{C}(P)\mathbf{A}_{\mathrm{F}}\sum_{\mathrm{F}}\mathbf{A}_{\mathrm{F}}{}^H\mathbf{C}^H(P) + \sigma_n{}^2\mathbf{I}_{(2L+1)\times(2L+1)} \end{aligned} \tag{15}$$

where $\mathbf{I}_{(2L+1)\times(2L+1)}$ is the $(2L+1)\times(2L+1)$ identity matrix, and $\sum_N$ and $\sum_F$ are diagonal matrices:

$$\sum_{N} = E\left\{\mathbf{S}_N(t)\,\mathbf{S}_N{}^H(t)\right\} \quad (16)$$

$$\sum_{F} = E\left\{\mathbf{S}_F(t)\,\mathbf{S}_F{}^H(t)\right\} \quad (17)$$

By implementing eigenvalue decomposition (EVD) of $\mathbf{R}$, the following equation holds:

$$\mathbf{R} = \mathbf{U}_s\mathbf{\Lambda}_s\mathbf{U}_s{}^H + \sigma_n{}^2\mathbf{U}_n\mathbf{U}_n{}^H \quad (18)$$

where $\mathbf{\Lambda}_s$ is the $K\times K$ diagonal matrix containing the K largest eigenvalues. In addition, $\mathbf{U}_n$ is the $(2L+1)\times(2L+1-K)$ matrix spanning the noise subspace of $\mathbf{R}$, and $\mathbf{U}_s$ is the $(2L+1)\times K$ matrix of $\mathbf{R}$ spanning the signal subspace.

As the fact that the MCM is a column full rank Toeplitz matrix, the authors can construct a MUSIC spectrum search function to estimate DOA and range parameters, and it is expressed as

$$p(\theta,r) = \mathbf{a}^H(\theta,r)\,\mathbf{C}^H(P)\,\mathbf{U}_n\mathbf{U}_n{}^H\mathbf{C}(P)\,\mathbf{a}(\theta,r) \quad (19)$$

From (19), it is obvious that the computational cost of this equation is unbearable with the unknown MCM. Even if MCM is accurately estimated as a prior, it requires a 2D spectrum search to estimate and match the DOA and range parameters pair as well. In order to decrease the huge computational cost, the DOA estimation of FF sources must be decoupled from mixed sources estimation and MCM.

According to the discussion of mutual coupling problem in [5], the following equation in ULA holds

$$\begin{aligned}\mathbf{C}(P)\,\mathbf{a}(\theta,r) &= \mathbf{B}(\theta,r)\,\mathbf{c}(P)\\ &= \mathbf{B}(\theta,r)\,\mathbf{E}(P)\left[1,\mathbf{c}_1{}^T(P)\right]^T\end{aligned} \quad (20)$$

where $\mathbf{B}(\theta,r) = \mathbf{B}_1 + \mathbf{B}_2$ is composed of two $(2L+1)\times(L+1)$ matrices, and they are defined as

$$\{\mathbf{B}_1\}_{p,q} = \begin{cases}[\mathbf{a}(\theta,r)]_{p+q-1}, & \text{for } p+q \le 2L+2\\ 0, & \text{otherwise}\end{cases} \quad (21)$$

$$\{\mathbf{B}_2\}_{p,q} = \begin{cases}[\mathbf{a}(\theta,r)]_{p-q+1}, & \text{for } p \ge q \ge 2\\ 0, & \text{otherwise}\end{cases} \quad (22)$$

$\mathbf{E}(P)$ denotes a $(L+1)\times(P+1)$ matrix defined as

$$\{\mathbf{E}(P)\}_{p,q} = \begin{cases}1, & \text{for } p = q\\ 0, & \text{otherwise}\end{cases} \qquad P = 0,1,\ldots,L-1 \quad (23)$$

where $\{\bullet\}_{p,q}$ represents the element corresponding to the p-th row and q-th column of the matrix, and $[\bullet]_p$ represents the element corresponding to p-th element of steering vector.

It is obvious that $\mathbf{U}_s$ and the combination of $\mathbf{C}(P)\mathbf{A}_N$ and $\mathbf{C}(P)\mathbf{A}_F$ can span the same signal subspace. Moreover, the signal subspace is orthogonal to the noise subspace spanned by $\mathbf{U}_n$. Therefore, the following equations hold:

$$\left|\mathbf{a}^H(\theta_k,r_k)\,\mathbf{C}^H\mathbf{U}_n\right|^2 = 0, \quad k = 1,\ldots K_1 \quad (24)$$

$$\left|\mathbf{a}^H(\theta_k,\infty)\,\mathbf{C}^H\mathbf{U}_n\right|^2 = 0, \quad k = 1+K_1,\ldots K \quad (25)$$

Therefore, based on (19), (20), and (25), the DOAs of FF sources can be estimated by the following spectrum search function:

$$\begin{aligned}&p(\theta,\infty,P)\\ &\quad = \mathbf{a}^H(\theta,\infty)\,\mathbf{C}(P)^H\,\mathbf{U}_n\mathbf{U}_n{}^H\mathbf{C}(P)\,\mathbf{a}(\theta,\infty)\\ &\quad = \left[1,\mathbf{c}_1{}^H(P)\right]\mathbf{E}^H(P)\,\mathbf{B}^H(\theta,\infty)\,\mathbf{U}_n\mathbf{U}_n{}^H\\ &\mathbf{B}(\theta,\infty)\,\mathbf{E}(P)\left[1,\mathbf{c}_1{}^T(P)\right]^T\\ &\quad = \left[1,\mathbf{c}_1{}^H(P)\right]\mathbf{W}(\theta,P)\left[1,\mathbf{c}_1{}^T(P)\right]^T\end{aligned} \quad (26)$$

where $\mathbf{W}(\theta,P)$ is defined as

$$\mathbf{W}(\theta,P) = \mathbf{E}^H(P)\,\mathbf{B}^H(\theta,\infty)\,\mathbf{U}_n\mathbf{U}_n{}^H\mathbf{B}(\theta,\infty)\,\mathbf{E}(P) \quad (27)$$

It must be noticed that $[1,\mathbf{c}_1{}^T(P)]^T \ne \mathbf{0}$ and $\mathbf{W}(\theta,P)$ is a nonnegative definite Hermite matrix. Based on the principle of RERA [29], $p(\theta,\infty,P)$ would be zero only when $\mathbf{W}(\theta,P)$ is a singular matrix. In other words, the determinant of $\mathbf{W}(\theta,P)$ would be equal to zero only when parameter P is greater than or equal to its accurate value P_{acc} and parameter θ is equal to any FF source's DOA θ_k ($k = 1+K_1,\ldots,K$). Consequently, P_{acc} and all the FF sources' DOAs can be estimated accurately by searching the K_2 highest spectrum peaks through the following function:

$$\begin{aligned}&p_F(\theta,P)\\ &\quad = \text{abs}\left\{\frac{1}{\det[\mathbf{W}(\theta,P)]} - \frac{1}{\det[\mathbf{W}(\theta,P-1)]}\right\}\\ &\qquad\qquad P = 1,2,\ldots,L-1\end{aligned} \quad (28)$$

where $\det[\bullet]$ signifies the determinant of a matrix and $\text{abs}\{\bullet\}$ denotes the absolute value of the element. From (28), it is easily seen that $p_F(\theta,P)$ is independently separated from (26). Therefore, the computational cost of DOAs estimating of FF sources through (28) is effectively reduced compared with the multidimensional MUSIC spectrum search function. It is because of that only a 2D spectrum search process is required.

It is noteworthy that the proposed algorithm woks in a similar way as that defined in [29, 30]. However, the algorithm in [29] only solves the problem of pure FF signals, whereas the proposed algorithm aims to deal with the problem of mixed FF and NF signals. Moreover, the algorithm in [30] solves the mixed sources problem with the accurate value of nonzero MCCs as prior knowledge. However, our work explicitly addresses mixed sources problem after blind calibration of the mutual coupling effect.

3.2. MCCs Estimation and MCM Reconstrucion. After estimating all DOAs of FF sources and accurate value P_{acc}, the MCCs are computed directly by the orthogonality between $\mathbf{C}(P_{acc})\mathbf{a}(\theta_k,\infty)$ $(k = K_1+1, K_1+2, \ldots, K)$ and $\mathbf{U}_{\rm n}$. According to (25), the following holds:

$$\begin{bmatrix} \mathbf{U}_{\rm n}{}^H \mathbf{C}(P_{acc})\mathbf{a}(\theta_{K_1+1},\infty) \\ \vdots \\ \mathbf{U}_{\rm n}{}^H \mathbf{C}(P_{acc})\mathbf{a}(\theta_{K},\infty) \end{bmatrix} = \mathbf{0}_{K_2(2L+1-K)\times 1} \tag{29}$$

where $\mathbf{0}_{K_2(2L+1-K)\times 1}$ denotes the $K_2(2L+1-K)\times 1$ zero vector. According to (20) and (25), (29) can be expressed as

$$\begin{aligned} &\begin{bmatrix} \mathbf{U}_{\rm n}{}^H \mathbf{B}(\theta_{K_1+1},\infty) \\ \vdots \\ \mathbf{U}_{\rm n}{}^H \mathbf{B}(\theta_{K},\infty) \end{bmatrix} \mathbf{E}(P_{acc})\mathbf{c}(P_{acc}) \\ &= \mathbf{H}\begin{bmatrix} 1 \\ \mathbf{c}_1(P_{acc}) \end{bmatrix} = \begin{bmatrix} \mathbf{H}_1 & \mathbf{H}_2 \end{bmatrix}\begin{bmatrix} 1 \\ \mathbf{c}_1(P_{acc}) \end{bmatrix} \\ &= \mathbf{0}_{K_2(2L+1-K)\times 1} \end{aligned} \tag{30}$$

where $\mathbf{H}_1$ is the first column of $\mathbf{H}$, and $\mathbf{H}_2$ is constructed of the rest P_{acc} columns. With replacing the DOA parameters in (30) by the FF sources' estimates, the least square solution of $\mathbf{c}_1$ can be obtained as

$$\mathbf{c}_1(P_{acc}) = -\left(\mathbf{H}_2{}^H\mathbf{H}_2\right)^{-1}\mathbf{H}_2{}^H\mathbf{H}_1 \tag{31}$$

According to the symmetric Toeplitz structure modeled in [5], the MCM can be reconstructed after nonzero MCCs have been calculated. Therefore, the reconstructed MCM can be used to eliminate the mutual coupling effect in the following signal processing process.

3.3. Mixed Sources Classification and NF Localization. After estimating $\mathbf{c}_1(P_{acc})$ and reconstructing the MCM, the mutual coupling effect can be eliminated effectively. We can get the received data vector without mutual coupling effect as follows:

$$\begin{aligned} \mathbf{Z}(t) &= \left[z_{-L}(t), z_{-L+1}(t), z_L(t)\right]^T = \mathbf{C}^{-1}(P_{acc})\mathbf{X}(t) \\ &= \mathbf{A}_{\rm N}\mathbf{S}_{\rm N}(t) + \mathbf{A}_{\rm F}\mathbf{S}_{\rm F}(t) + \mathbf{C}^{-1}(P_{acc})\mathbf{N}(t) \end{aligned} \tag{32}$$

As the discussion in Section 2, it is obvious that the common characteristic of NF and FF sources is α_k and the differences are that β_k is approximately equal to zero for FF source but nonzero for NF source. It shows a way that we can construct some matrices which only contain the common term α_k no matter whether these sources are NF sources or FF sources. In this way, the common term α_k existing in both FF and NF sources can be estimated by the conventional high-resolution algorithms.

As is known, HOC technique can generate the virtual array to improve the estimation accuracy [32]. In addition, the cumulant of Gaussian random process is equal to zero when the order of cumulant is greater than second [33]. This property can be used to eliminate the effect of additive colored Gaussian noise caused by blind calibration in (32). Consequently, FOC technique is chosen as a key technique in this subsection.

The symmetry definition of FOC of the zero-mean stationary random process can be given as follows:

$$\begin{aligned} &\operatorname{cum}\left(z_i(t), z_p(t), z_q^*(t), z_j^*(t)\right) \\ &= \operatorname{cum}\Bigg(\sum_{k=1}^{K} e^{j(\alpha_k i+\beta_k i^2)} s_k(t), \sum_{k=1}^{K} e^{j(\alpha_k p+\beta_k p^2)} s_k(t), \\ &\quad \sum_{k=1}^{K} e^{-j(\alpha_k q+\beta_k q^2)} s_k^*(t), \sum_{k=1}^{K} e^{-j(\alpha_k j+\beta_k j^2)} s_k^*(t)\Bigg) \\ &\quad + \operatorname{cum}\left(n_i(t), n_p(t), n_q^*(t), n_j^*(t)\right) \\ &= \sum_{k=1}^{K} e^{j\alpha_k[(i-q)-(j-p)]+j\beta_k[(i^2-q^2)-(j^2-p^2)]}\gamma_k \\ &\qquad i, j, p, q \in \{-L, -L+1, \ldots, L\} \end{aligned} \tag{33}$$

where $\gamma_k = \operatorname{cum}(s_k(t), s_k(t), s_k{}^*(t), s_k{}^*(t))$ is the kurtosis of the k-th signal, and i, j, p, q are the indexes of sensors.

Based on the above observation, a $2L\times 2L$ FOC matrix $\mathbf{F}_1$ containing only the data received by the first $2L$ sensors can be defined as

$$\begin{aligned} &\mathbf{F}_1(L+1+i, L+1+j) \\ &= \operatorname{cum}\left(z_i(t), z_{-1-j}(t), z_{-1-i}^*(t), z_j^*(t)\right) \\ &= \sum_{k=1}^{K} e^{j(\alpha_k-\beta_k)[(2i+1)-(2j+1)]}\gamma_k \\ &\qquad i, j \in \{-L, -L+1, \ldots, L-1\}. \end{aligned} \tag{34}$$

Similarly, another $2L\times 2L$ FOC matrix $\mathbf{F}_2$ containing only the data received the last $2L$ sensors that can be given by

$$\begin{aligned} &\mathbf{F}_2(L+i, L+j) \\ &= \operatorname{cum}\left(z_i(t), z_{1-j}(t), z_{1-i}^*(t), z_j^*(t)\right) \\ &= \sum_{k=1}^{K} e^{j(\alpha_k+\beta_k)[(2i-1)-(2j-1)]}\gamma_k \\ &\qquad i, j \in \{-L+1, -L+2, \ldots, L\} \end{aligned} \tag{35}$$

In order to construct a Hermite matrix, a cross-correlation matrix of the two subarrays is needed which is defined as matrix $\mathbf{F}_3$. The matrix $\mathbf{F}_3$ is the cross FOC matrix of the two subarrays, actually.

$$\begin{aligned}\mathbf{F}_3(L+1+i, L+j) &= \operatorname{cum}\left(z_i(t), z_{1-j}(t), z^*_{-1-i}(t), z^*_j(t)\right) \\ &= \sum_{k=1}^{K} e^{j(\alpha_k-\beta_k)(2i+1)} e^{-j(\alpha_k+\beta_k)(2j-1)} \gamma_k \\ i \in \{-L, -L+1, \ldots, L-1\}, &\quad j \in \{-L+1, -L+2, \ldots, L\}\end{aligned} \tag{36}$$

And then, a $4L \times 4L$ Hermite matrix constructed by the three FOC matrices is described as

$$\mathbf{F} = \begin{bmatrix} \mathbf{F}_1 & \mathbf{F}_3^H \\ \mathbf{F}_3 & \mathbf{F}_2 \end{bmatrix} \tag{37}$$

It must be noticed that the matrix $\mathbf{F}$ can be expressed in a compact matrix form

$$\mathbf{F} = \mathbf{G}\mathbf{F}_\gamma \mathbf{G}^H \tag{38}$$

where $\boldsymbol{F}_\gamma = \operatorname{diag}[\gamma_1, \gamma_2, \ldots, \gamma_K]$ and $\mathbf{G}$ denotes the $4L \times K$ steering matrix of $\mathbf{F}$. In this way, the steering matrix $\mathbf{G}$ can be divided into two parts.

$$\mathbf{G} = \left[\mathbf{G}_1{}^T, \mathbf{G}_2{}^T\right]^T \tag{39}$$

where $\mathbf{G}_1$ and $\mathbf{G}_2$ are two $2L \times K$ steering matrices, which can be expressed as

$$\mathbf{G}_1 = \begin{bmatrix} e^{j(\alpha_1-\beta_1)(-2L+1)} & e^{j(\alpha_2-\beta_2)(-2L+1)} & \cdots & e^{j(\alpha_K-\beta_K)(-2L+1)} \\ e^{j(\alpha_1-\beta_1)(-2L+3)} & e^{j(\alpha_2-\beta_2)(-2L+3)} & \cdots & e^{j(\alpha_K-\beta_K)(-2L+3)} \\ \vdots & \vdots & \ddots & \vdots \\ e^{j(\alpha_1-\beta_1)(2L-1)} & e^{j(\alpha_2-\beta_2)(2L-1)} & \cdots & e^{j(\alpha_K-\beta_K)(2L-1)} \end{bmatrix} \tag{40}$$

$$\mathbf{G}_2 = \begin{bmatrix} e^{j(\alpha_1+\beta_1)(-2L-1)} & e^{j(\alpha_2+\beta_2)(-2L-1)} & \cdots & e^{j(\alpha_K+\beta_K)(-2L-1)} \\ e^{j(\alpha_1+\beta_1)(-2L+1)} & e^{j(\alpha_2+\beta_2)(-2L+1)} & \cdots & e^{j(\alpha_K+\beta_K)(-2L+1)} \\ \vdots & \vdots & \ddots & \vdots \\ e^{j(\alpha_1+\beta_1)(2L+1)} & e^{j(\alpha_2+\beta_2)(2L+1)} & \cdots & e^{j(\alpha_K+\beta_K)(2L+1)} \end{bmatrix} \tag{41}$$

By implementing EVD of $\mathbf{F}$, the following holds:

$$\mathbf{F} = \mathbf{V}\boldsymbol{\Sigma}\mathbf{V}^H \tag{42}$$

where $\boldsymbol{\Sigma}$ is the $K \times K$ diagonal matrix containing only the nonzero eigenvalues, and $\mathbf{V}$ is the $4L \times K$ matrix composed of eigenvectors spanning the signal subspace of $\mathbf{F}$.

Similarly, $\mathbf{V}$ can be divided into two matrices as well.

$$\mathbf{V} = \left[\mathbf{V}_1{}^T, \mathbf{V}_2{}^T\right]^T \tag{43}$$

where $\mathbf{V}_1$ and $\mathbf{V}_2$ are two $2L \times K$ matrices.

It is obvious that $\mathbf{V}$ and $\mathbf{G}$ span the same signal subspace of $\mathbf{F}$. In order to avoid any spatial spectrum search, the matrices $\mathbf{V}_1$, $\mathbf{V}_2$, $\mathbf{G}_1$, and $\mathbf{G}_2$ are divided as follows:

$$\mathbf{V}_1 = \begin{bmatrix} \mathbf{V}_{1,F} \\ \textit{last row} \end{bmatrix} = \begin{bmatrix} \textit{first row} \\ \mathbf{V}_{1,B} \end{bmatrix} \tag{44a}$$

$$\mathbf{V}_2 = \begin{bmatrix} \mathbf{V}_{2,F} \\ \textit{last row} \end{bmatrix} = \begin{bmatrix} \textit{first row} \\ \mathbf{V}_{2,B} \end{bmatrix} \tag{44b}$$

$$\mathbf{G}_1 = \begin{bmatrix} \mathbf{G}_{1,F} \\ \textit{last row} \end{bmatrix} = \begin{bmatrix} \textit{first row} \\ \mathbf{G}_{1,B} \end{bmatrix} \tag{45a}$$

$$\mathbf{G}_2 = \begin{bmatrix} \mathbf{G}_{2,F} \\ \textit{last row} \end{bmatrix} = \begin{bmatrix} \textit{first row} \\ \mathbf{G}_{2,B} \end{bmatrix} \tag{45b}$$

As the fact that $\mathbf{V}_1$ and $\mathbf{V}_2$ are column full rank matrices, two transformation matrices $\boldsymbol{\Psi}_1$ and $\boldsymbol{\Psi}_2$ can be estimated by

$$\boldsymbol{\Psi}_1 == \mathbf{T}^{-1}\boldsymbol{\Phi}_1\mathbf{T} = \left(\mathbf{V}_{1,F}{}^H\mathbf{V}_{1,F}\right)^{-1} \mathbf{V}_{1,F}{}^H\mathbf{V}_{1,B} \tag{46}$$

$$\boldsymbol{\Psi}_2 = \mathbf{T}^{-1}\boldsymbol{\Phi}_2\mathbf{T} = \left(\mathbf{V}_{2,F}{}^H\mathbf{V}_{2,F}\right)^{-1} \mathbf{V}_{2,F}{}^H\mathbf{V}_{2,B} \tag{47}$$

where $\mathbf{T}$ is a unknown $K \times K$ full rank transformation matrix. $\boldsymbol{\Phi}_1$ and $\boldsymbol{\Phi}_2$ are $K \times K$ diagonal matrices expressed as

$$\boldsymbol{\Phi}_1 = \operatorname{diag}\left[e^{j2(\alpha_1-\beta_1)}, e^{j2(\alpha_2-\beta_2)}, \ldots, e^{j2(\alpha_K-\beta_K)}\right] \tag{48}$$

$$\boldsymbol{\Phi}_2 = \operatorname{diag}\left[e^{j2(\alpha_1+\beta_1)}, e^{j2(\alpha_2+\beta_2)}, \ldots, e^{j2(\alpha_K+\beta_K)}\right] \tag{49}$$

Thus, α_k and β_k can be estimated by implementing EVD of $\boldsymbol{\Psi}_1$ and $\boldsymbol{\Psi}_2$ [1].

It must be noticed that $\boldsymbol{\Phi}_1(k,k) = \boldsymbol{\Phi}_2(k,k)$ only when the k-th source is FF source. Thus, this algorithm can deal with the problem of mixed sources classification efficiently.

It is undeniable that the following algebraic expression can be used to estimate θ_k

$$\widehat{\theta}_k = \arcsin\left(\frac{\arg\left[\boldsymbol{\Phi}_1(k,k)\,\boldsymbol{\Phi}_2(k,k)\right]}{-8\pi d/\lambda}\right) \tag{50}$$

After implementing DOAs estimation of all sources and sources classification, the range parameter of any NF source can be calculated by

$$\widehat{r}_k = \frac{4\pi d^2 \cos\left(\widehat{\theta}_k\right)/\lambda}{\arg\left[\boldsymbol{\Phi}_2(k,k)/\boldsymbol{\Phi}_1(k,k)\right]} \tag{51}$$

3.4. The Proposed Algorithm Summary. In the above description, the authors introduce the proposed algorithm process based on the ideal model. However, in practice, it is almost impossible to calculate ideal covariance matrix or FOC one. Hence in algorithm execution process, $\mathbf{R}$ and $\mathbf{F}$ must be replaced by the estimated ones with limited snapshots sample.

Consequently, the proposed algorithm can be summarized as follows.

Step 1. Estimate the covariance matrix through (15).

Step 2. Implement EVD of covariance matrix $\mathbf{R}$ to generate its noise subspace.

Step 3. Estimate the DOAs of FF sources and parameter P through (28).

Step 4. Obtain the MCCs by (31), and construct the MCM by (6).

Step 5. Compensate the MCM by (32).

Step 6. Construct the FOC matrix $\mathbf{F}$ by (34)-(37).

Step 7. Implement EVD of $\mathbf{F}$ to generate its signal subspace.

Step 8. Compute the two transformation matrices by (46) and (47), and implement EVD of them to obtain the two diagonal matrices $\mathbf{\Phi}_1$ and $\mathbf{\Phi}_2$.

Step 9. Estimate the parameter of NF sources through (50) and (51) .

3.5. Discussion

3.5.1. Array Configuration and MCCs Parameter. As is known that the amplitude of MCCs is in inverse proportion to the physical distance between each pair of sensors, it means that number of nonzero MCCs defined as P_{acc} would be constant even if the number of array elements is infinite.

In order to estimate the correct MCCs by rank-reduction technique without ambiguity, the minimum number of array elements must be set as $2P_{acc}+3$. However, the accurate value P_{acc} is unknown before it is estimated. Therefore, a large number of array elements are required to guarantee the effective estimation of P_{acc}. After MCCs being estimated, we can arbitrarily adjust the size of the array to reduce the unnecessary array redundancy.

3.5.2. Number of Required Array Elements. In order to get the unique solution of (28), $\mathbf{W}(\theta, P)$ must be invertible at nonincident direction; that is,

$$\operatorname{rank}\left(\mathbf{B}(\theta,\infty)\,\mathbf{E}(P)\right) \le \operatorname{rank}\left(\mathbf{U}_{\mathrm{n}}\mathbf{U}_{\mathrm{n}}{}^{H}\right) \tag{52}$$

Furthermore, as the assumption in Section 2, the rank of $\mathbf{U}_{\mathrm{n}}\mathbf{U}_{\mathrm{n}}{}^{H}$ is $2L+1-K$ and the maximum rank of $\mathbf{B}(\theta,\infty)\mathbf{E}(P)$ may be L. Hence, the parameter identifiability condition of the algorithm is $K \le L+1$.

3.5.3. Computational Complexity. In the interest of computational complexity comparison, the Cum4MUSIC algorithm and TSMUSIC algorithm are set as comparison objects of the proposed algorithm. For all three algorithms, the major computation processes are calculating statistical matrices, eigenvalue decomposing, and spectrum searching. It is defined that the search step of azimuth $\theta \in [-90^\circ, 90^\circ]$ is θ_Δ and that of $r \in [0.62(D^3/\lambda)^{1/2}, 2D^2/\lambda]$ is r_Δ for K_1 NF sources. We assume that N is the number of snapshots.

For Cum4MUSIC algorithm the major computations are to form two $(2L+1)\times(2L+1)$ matrices and to implement the EVDs of the two matrices for spatial searching twice. Thus, the computational complexity of Cum4MUSIC algorithm is

$$\begin{aligned} &18\,(2L+1)^2 N + \frac{8}{3}(2L+1)^3 + 2\frac{180\,(2L+1)^2}{\theta_\Delta} \\ &\quad + K_1 \frac{2D^2/\lambda - 0.62\left(D^3/\lambda\right)^{1/2}}{r_\Delta}(2L+1)^2 \end{aligned} \tag{53}$$

For TSMUSIC algorithm the major computations are to form a $(2L+1)\times(2L+1)$ covariance matrix and a $(2L+1)\times(2L+1)$ noise subspace matrix and to implement EVD of the covariance matrix. After that, three times of spatial searching are required to estimate the DOAs of NF and FF sources and the ranges of NF sources, respectively. Thus, the computational complexity of this algorithm is

$$\begin{aligned} &(2L+1)^2 (N+1) + \frac{4}{3}(2L+1)^3 + 2\frac{180\,(2L+1)^2}{\theta_\Delta} \\ &\quad + K_1 \frac{2D^2/\lambda - 0.62\left(D^3/\lambda\right)^{1/2}}{r_\Delta}(2L+1)^2 \end{aligned} \tag{54}$$

For the algorithm in [30] the major computations are to form $(2L+1)\times(2L+1)$ covariance matrices and to implement EVD of them. After that, three times of spatial searching are required to estimate the DOAs of NF and FF sources and the ranges of NF sources, respectively. Thus, the computational complexity of this algorithm is

$$\begin{aligned} &(2L+1)^2 N + \frac{8}{3}(2L+1)^3 + 2\frac{180\,(2L+1)^2}{\theta_\Delta} \\ &\quad + K_1 \frac{2D^2/\lambda - 0.62\left(D^3/\lambda\right)^{1/2}}{r_\Delta}(2L+1)^2 \end{aligned} \tag{55}$$

The proposed algorithm requires a SOC matrix and a FOC one. The major computations are to implement EVD of the $L\times L$ SOC matrix and to implement L times spatial searching. Besides, implementing EVDs of the $4L\times 4L$ FOC matrix and another two $(2L-1)\times(2L-1)$ matrices are required as well. Thus, the computational complexity of proposed algorithm is

$$\begin{aligned} &9\,(2L+1)^2 N + 3\,(2L)^2 N + \frac{4}{3}(4L)^3 + \frac{8}{3}(2L-1)^3 \\ &\quad + \frac{180\,(2L+1)^2}{\theta_\Delta} L \end{aligned} \tag{56}$$

3.5.4. Capacity for Classification Mixed Sources. From the above analysis, it is obvious that if the FF sources and the NF sources have the same DOA, Cum4MUSIC algorithm would be invalid. Compared with the above-mentioned algorithm, TSMUSIC algorithm can eliminate FF components when estimating only NF sources. However, it ignores the mutual

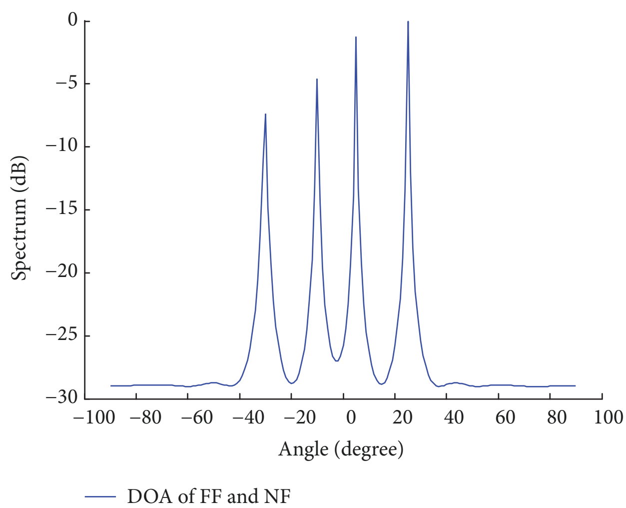

Figure 2: DOA spectra of Cum4MUSIC.

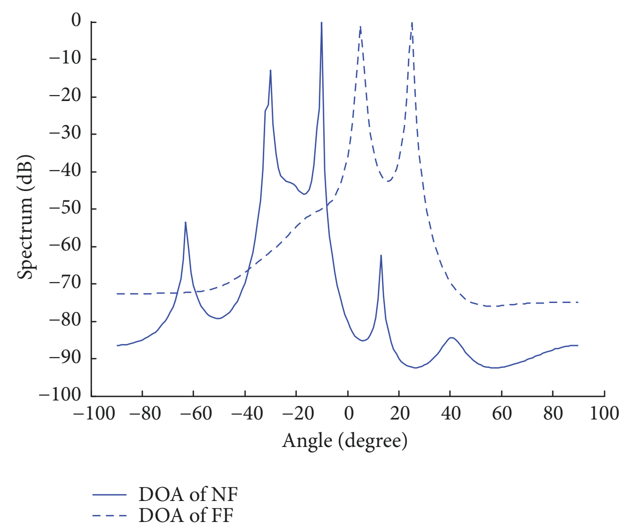

Figure 3: DOA spectra of TSMUSIC.

coupling effect. Fortunately, the proposed algorithm can implement the mixed sources classification under mutual coupling, through the differences between the corresponding elements of two diagonal matrices.

4. Simulation Results

Some simulations are conducted in this section to evaluate the proposed algorithm. A ULA of 11 elements is taken into consideration. The input signal to noise ratio (SNR) of the k-th source is defined as $10 \times \log_{10}(\sigma_k^2/\sigma_n^2)$, where σ_k^2 denotes the power of the k-th source, and σ_n^2 denotes the noise power. It is assumed that all sources are with equal power. In the following experiments, the performance is measured by the root mean square errors (RMSE) of 100 independent Monte Carlo experiments.

It is noticed that the estimation performance of the range parameter is only for NF sources experiment but not for FF sources experiment.

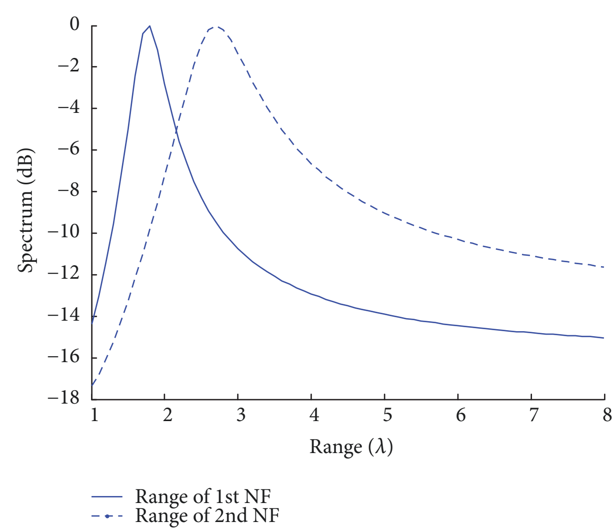

Figure 4: Range spectra of TSMUSIC.

4.1. Spectra of DOA and Range Estimation in Presence of Mutual Coupling Effect. In the first simulation, the authors consider a scenario where two NF sources and two FF sources coexist, and they are located at $\{\theta_1 = -30^\circ, r_1 = 1.7\lambda\}$, $\{\theta_2 = -10^\circ, r_2 = 2.6\lambda\}$, $\{\theta_3 = 5^\circ, r_3 = \infty\}$, and $\{\theta_4 = 25^\circ, r_4 = \infty\}$. The number of snapshots is set as 200 and the SNR of incoming sources is set as 10 dB. In addition, the nonzero MCCs are set as $[1, -0.0886 + 0.0464i, 0.0067 - 0.0075i]$ with $P_{acc} = 2$.

The DOA and range spectra of the four algorithms are shown from Figures 2–9. From Figure 2, it is shown that Cum4MUSIC generates four highest sharp spectrum peaks on the directions of NF and FF sources. It must be noted that Cum4MUSIC fails to classify NF sources between the mixed sources. Therefore, its range estimation would be invalid.

From Figure 3, it is shown that TSMUSIC algorithm generates worse spectrum of NF sources than that in Figure 2. Moreover, there are other false peaks caused by the unknown mutual coupling effect, which would lead to false estimation. This is because that TSMUSIC cannot eliminate the FF components under unknown mutual coupling. Therefore, the mutual coupling effect and the propagated error of DOA estimation lead to reliable range parameters estimation as shown in Figure 4.

In Figure 5, it shows that the algorithm in [30] generates different DOA spectra with different parameter P. From Figure 6, it is shown that the DOA estimates of NF sources have significant estimating error when the algorithm sets P with a wrong value. As a result, the propagation error of NF sources estimates would degrade the performance of range estimation as shown in Figure 7.

From Figure 8, it is shown that the proposed algorithm generates two sharp peaks in the spectra of FF sources with different value of parameter P. In addition, it obviously shows that the shark peaks have an almost equal amplitude when

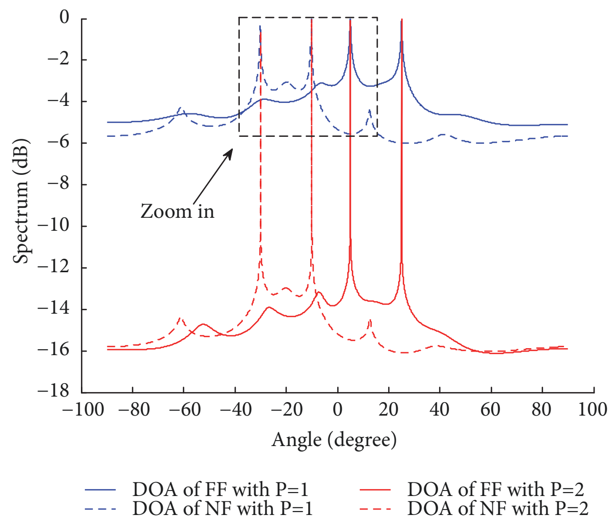

FIGURE 5: DOA spectra of algorithm in [30].

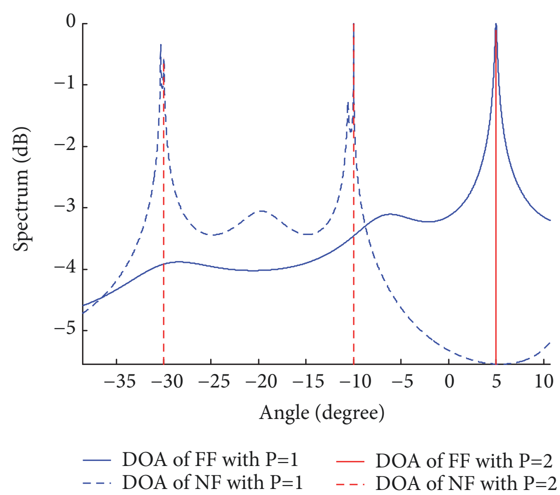

FIGURE 6: Local enlarged drawing of Figure 5.

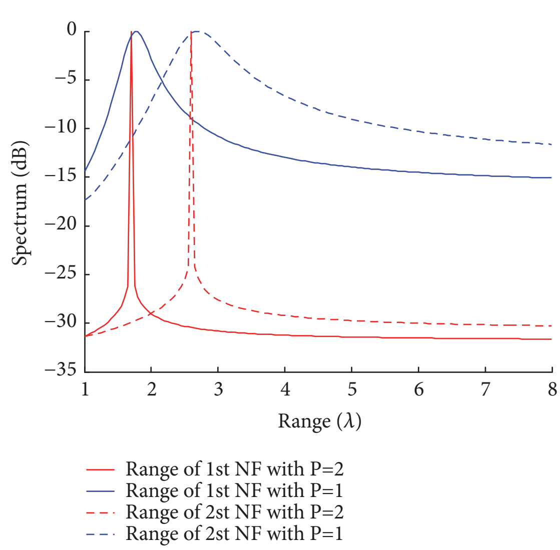

FIGURE 7: Range spectra of the algorithm in [30].

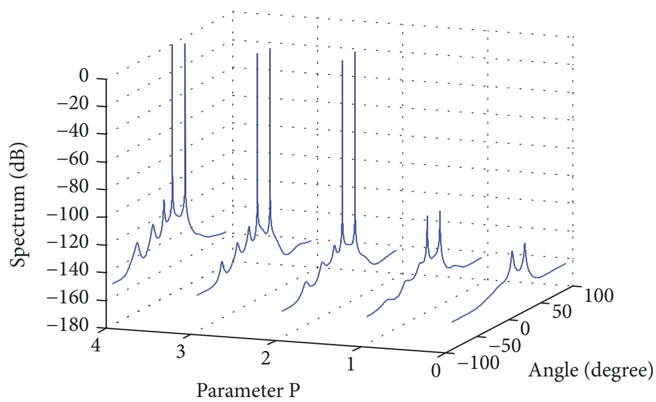

Figure 8: DOA spectra of proposed algorithm with different parameter P.

Table 1: NF sources estimates of proposed algorithm.

Source No.	DOA/degree	Range/λ
1st NF source	-30.0061	1.7015
2nd NF source	-10.0039	2.6001

the value of parameter P is greater than or equal to P_{acc}. The spectrum of FF DOA and parameter P is shown in Figure 9. The proposed algorithm generates two sharp peaks on the cross points of FF sources' directions and P_{acc}. The range parameter of the proposed algorithm is estimated without spectrum searching, so that it is inconvenient to give any range spectrum. Therefore, the authors give the DOAs and ranges estimation results of NF sources in Table 1.

As a result, the DOA estimates of Cum4MUSIC and TSMUSIC are biased due to the unknown mutual coupling effect. The algorithm in [30] must work with the accurate value of P. However, this algorithm always works without parameter P estimation. Moreover, the proposed algorithm can achieve better range estimates of the two NF sources than those estimated by TSMUSIC.

4.2. Performance versus Snapshot Number in Presence of Mutual Coupling Effect. In the second simulation, the authors consider a scenario in where one NF source and one FF source coexist, and the location parameters are $\{\theta_5 = -17^\circ, r_5 = 2.2\lambda\}$ and $\{\theta_6 = 23^\circ, r_6 = \infty\}$, with the SNR being set as 10dB. The nonzero MCCs are set as the same as those in the first experiment and the number of snapshots varies from 100 to 1000.

The RMSEs of the DOA and range estimates, as the snapshot number changes, are shown in Figures 10 and 11. It obviously shows that both the DOA and the range estimation RMSEs of the proposed algorithm decrease monotonically as the snapshot number increases. It is due to the fact that a larger sampling number will produce better estimates of the cumulant matrices. In addition, the FF DOA estimation of algorithm in [30] has equivalent performance with the proposed one. However, the proposed algorithm gains the better performances of NF DOA and range estimation than that in [30]. Compared with the proposed algorithm, both the DOA and range RMSEs of Cum4MUSIC and TSMUSIC algorithms no longer decrease as the number of snapshots increases due to the steering mismatching caused by mutual coupling effect.

4.3. Performance versus SNR in Presence of Mutual Coupling Effect. In the third simulation, almost all simulation conditions are adopted as the same as those in the second experiment except that the number of snapshots is set as 200 and the SNR varies from −5 dB to 20 dB.

The RMSEs of the DOA and range estimates, as the changes of SNR, are shown from Figures 12 and 13. In Figure 12, it shows that the algorithm in [30] has equivalent FF DOA estimation performance with the proposed algorithm. However, the proposed algorithm gains the better performances of NF DOA estimation. As a result, the proposed algorithm outperforms the other three algorithms in both DOA and range estimation in Figure 10. Moreover, the increasing SNR is no longer helpful for Cum4MUSIC and TSMUSIC due to the model errors of cumulant matrices caused by the dominating unknown mutual coupling effect.

4.4. Computational Complexity Comparison. In the last experiment, we compare the computational complexity of the four algorithms. Suppose that there are $2L + 1 = 11$ sensors, and the searching steps are as $\theta_\Delta = 0.1^\circ$ and $r_\Delta = 0.02\lambda$, respectively. The number of snapshots varies from 100 to1000. Furthermore, we define $K = 4$, $K_1 = 2$, $K_2 = 2$. In Figure 14, it illustrates the computational burden of these four algorithms as a function of the snapshot number. It is clear that the proposed algorithm has the minimum computational complexity since it avoids any NF DOA and range spectra searching.

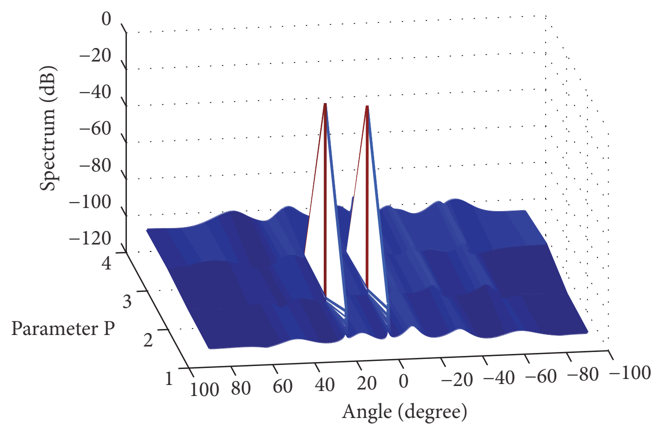

Figure 9: DOA and parameter P spectrum of proposed algorithm.

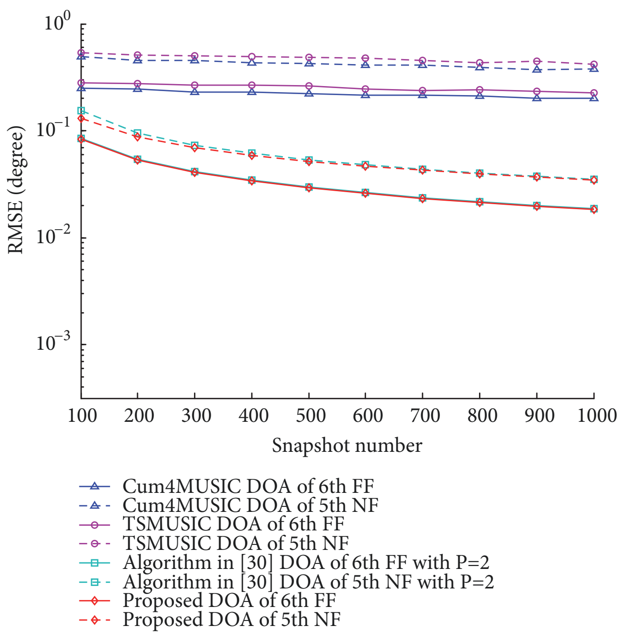

Figure 10: RMSEs of the DOA estimates versus snapshot number.

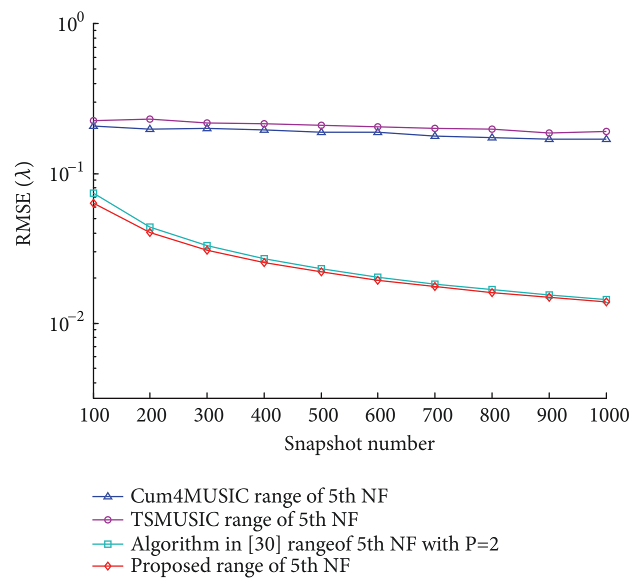

Figure 11: RMSEs of the range estimates versus snapshot number.

5. Conclusions

In this paper, a high performance algorithm for mixed NF and FF sources classification and localization after blind calibration of unknown mutual coupling is proposed. Compared with aforementioned algorithms, the proposed algorithm is effective in mixed sources classification and localization as well as mutual coupling parameter estimation. Moreover, it can provide better DOA and range estimation performance under the mutual coupling effect. On one hand, for computational complexity, the proposed algorithm successfully avoids multidimensional spectrum search (with respect to MCCs and range) and parameter matching. Finally, many simulation results give forceful proof of that the proposed algorithm is efficient for the problem of mixed sources classification and localization under unknown mutual coupling. On the other hand, in many references, the mutual coupling effect is usually modeled as a symmetric Toeplitz matrix simply with a known number of nonzero MCCs. However, in practice, it is much more complicated due to the complex microwave propagation environment. Fortunately, the proposed algorithm successfully estimates the number of nonzero MCCs firstly, which would affect the estimation performance. As a result, in order to estimate the number of nonzero MCCs accurately, there should be enough sensors located in the array at the beginning. After MCCs being estimated, the size of array can be adjusted freely.

Data Availability

The simulation data used to support the findings of this study are included within the article.

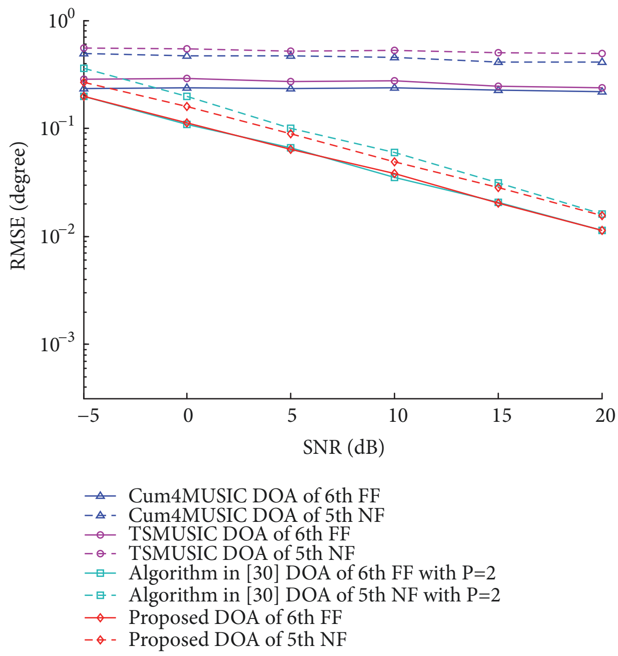

Figure 12: RMSEs of the DOA estimates versus SNR.

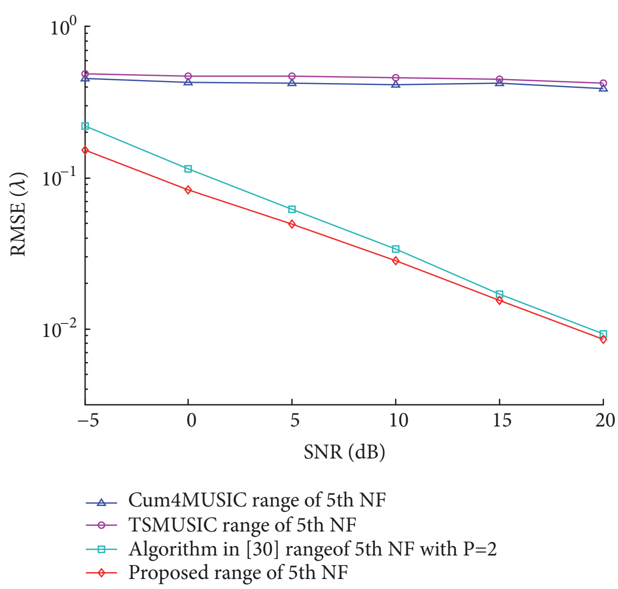

Figure 13: RMSEs of the range estimates versus SNR.

Conflicts of Interest

The authors declare no conflicts of interest.

Acknowledgments

This work was supported by the National Key Research and Development Program of China under Grant no. 2018YFB0505104 and by the National Natural Science Foundation of China under Grant nos. 61601372 and 61771404.

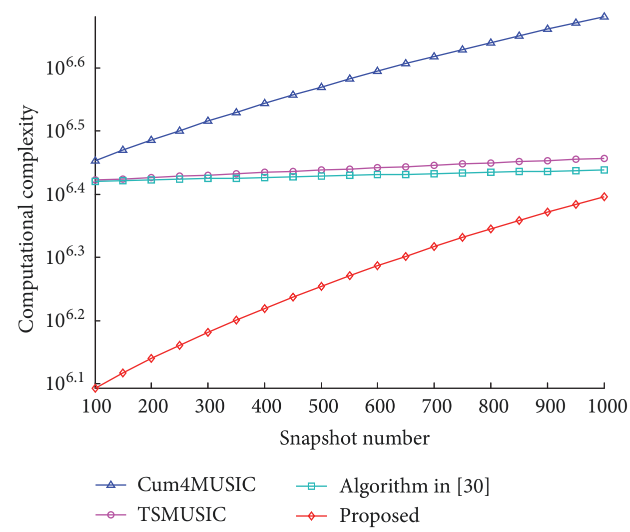

Figure 14: Computational complexities of the four methods versus snapshot number.

References

[1] R. Roy and T. Kailath, "ESPRIT-estimation of signal parameters via rotational invariance techniques," *IEEE Transactions on Signal Processing*, vol. 37, no. 7, pp. 984–995, 1989.

[2] M. Cao, L. Huang, C. Qian, J. Xue, and H. So, "Underdetermined DOA estimation of quasi-stationary signals via Khatri–Rao structure for uniform circular array," *Signal Processing*, vol. 106, pp. 41–48, 2015.

[3] R. Schmidt, "Multiple emitter location and signal parameter estimation," *IEEE Transactions on Antennas and Propagation*, vol. 34, no. 3, pp. 276–280, 1986.

[4] C. Qian, L. Huang, and H. So, "Computationally efficient ESPRIT algorithm for direction-of-arrival estimation based on Nyström method," *Signal Processing*, vol. 94, pp. 74–80, 2014.

[5] Y. Wang, M. Trinkle, and B. Ng, "DOA Estimation under Unknown Mutual Coupling and Multipath with Improved Effective Array Aperture," *Sensors*, vol. 15, no. 12, pp. 30856–30869, 2015.

[6] Y. D. Huang and M. Barkat, "Near-field multiple source localization by passive sensor array," *IEEE Transactions on Antennas and Propagation*, vol. 39, no. 7, pp. 968–975, 1991.

[7] W. Zhi and M. Y.-W. Chia, "Near-field source localization via symmetric subarrays," *IEEE Signal Processing Letters*, vol. 14, no. 6, pp. 409–412, 2007.

[8] J. He, M. O. Ahmad, and M. N. Swamy, "Near-Field Localization of Partially Polarized Sources with a Cross-Dipole Array," *IEEE Transactions on Aerospace and Electronic Systems*, vol. 49, no. 2, pp. 857–870, 2013.

[9] J.-W. Tao, L. Liu, and Z.-Y. Lin, "Joint DOA, range, and polarization estimation in the fresnel region," *IEEE Transactions on Aerospace and Electronic Systems*, vol. 47, no. 4, pp. 2657–2672, 2011.

[10] J. Xie, H. Tao, X. Rao, and J. Su, "Efficient Method of Passive Localization for Near-Field Noncircular Sources," *IEEE Antennas and Wireless Propagation Letters*, vol. 14, pp. 1223–1226, 2015.

[11] J. Su, J. Xie, X. Rao, and H. Tao, "Real-valued localisation algorithm for near-field non-circular sources," *IEEE Electronics Letters*, vol. 51, no. 17, pp. 1330-1331, 2015.

[12] J. Lee, Y. Chen, and C. Yeh, "Covariance approximation method for near-field direction-finding using a uniform linear array," *IEEE Transactions on Signal Processing*, vol. 43, no. 5, pp. 1293–1298, 1995.

[13] H. Noh and C. Lee, "A covariance approximation method for near-field coherent sources localization using uniform linear array," *IEEE Journal of Oceanic Engineering*, vol. 40, no. 1, pp. 187–195, 2015.

[14] E. Grosicki, K. Abed-Meraim, and Y. Hua, "A weighted linear prediction method for near-field source localization," *IEEE Transactions on Signal Processing*, vol. 53, no. 10, pp. 3651–3660, 2005.

[15] J. Liang and D. Liu, "Passive localization of near-field sources using cumulant," *IEEE Sensors Journal*, vol. 9, no. 8, pp. 953–960, 2009.

[16] J. Liang and D. Liu, "Passive localization of mixed near-field and far-field sources using two-stage music algorithm," *IEEE Transactions on Signal Processing*, vol. 58, no. 1, pp. 108–120, 2010.

[17] J. He, M. N. Swamy, and M. O. Ahmad, "Efficient application of music algorithm under the coexistence of far-field and near-field sources," *IEEE Transactions on Signal Processing*, vol. 60, no. 4, pp. 2066–2070, 2012.

[18] B. Wang, J. Liu, and X. Sun, "Mixed sources localization based on sparse signal reconstruction," *IEEE Signal Processing Letters*, vol. 19, no. 8, pp. 487–490, 2012.

[19] B. Wang, Y. Zhao, and J. Liu, "Mixed-order MUSIC algorithm for localization of far-field and near-field sources," *IEEE Signal Processing Letters*, vol. 20, no. 4, pp. 311–314, 2013.

[20] G. Liu and X. Sun, "Two-stage matrix differencing algorithm for mixed far-field and near-field sources classification and localization," *IEEE Sensors Journal*, vol. 14, no. 6, pp. 1957–1965, 2014.

[21] X. Sun, G. Liu, Y. Qin, and Y. Liu, "Low-complexity estimation of signal parameters via rotational invariance techniques algorithm for mixed far-field and near-field cyclostationary sources localisation," *IET Signal Processing*, vol. 7, no. 5, pp. 382–388, 2013.

[22] J. Jiang, F. Duan, J. Chen, Y. Li, and X. Hua, "Mixed near-field and far-field sources localization using the uniform linear sensor array," *IEEE Sensors Journal*, vol. 13, no. 8, pp. 3136–3143, 2013.

[23] G. Li, S. Yang, and Z. Nie, "Direction of arrival estimation in time modulated linear arrays with unidirectional phase center motion," *IEEE Transactions on Antennas and Propagation*, vol. 58, no. 4, pp. 1105–1111, 2010.

[24] Z. Ye, J. Dai, X. Xu, and X. Wu, "DOA estimation for uniform linear array with mutual coupling," *IEEE Transactions on Aerospace and Electronic Systems*, vol. 45, no. 1, pp. 280–288, 2009.

[25] X. Xu, Z. Ye, and Y. Zhang, "DOA estimation for mixed signals in the presence of mutual coupling," *IEEE Transactions on Signal Processing*, vol. 57, no. 9, pp. 3523–3532, 2009.

[26] C. Liu, Z. Ye, and Y. Zhang, "DOA estimation based on fourth-order cumulants with unknown mutual coupling," *Signal Processing*, vol. 89, no. 9, pp. 1839–1843, 2009.

[27] R. Goossens and H. Rogier, "A hybrid UCA-RARE/Root-MUSIC approach for 2-D direction of arrival estimation in uniform circular arrays in the presence of mutual coupling," *IEEE Transactions on Antennas and Propagation*, vol. 55, no. 3, pp. 841–849, 2007.

[28] C. Qi, Y. Wang, Y. Zhang, and H. Chen, "DOA estimation and self-calibration algorithm for uniform circular array," *IEEE Electronics Letters*, vol. 41, no. 20, p. 1092, 2005.

[29] M. Lin and L. Yang, "Blind calibration and DOA estimation with uniform circular arrays in the presence of mutual coupling," *IEEE Antennas and Wireless Propagation Letters*, vol. 5, no. 1, pp. 315–318, 2006.

[30] J. Xie, H. Tao, X. Rao, and J. Su, "Localization of mixed far-field and near-field sources under unknown mutual coupling," *Digital Signal Processing*, vol. 50, pp. 229–239, 2016.

[31] N. Yuen and B. Friedlander, "Performance analysis of higher order ESPRIT for localization of near-field sources," *IEEE Transactions on Signal Processing*, vol. 46, no. 3, pp. 709–719, 1998.

[32] M. C. Dogan and J. M. Mendel, "Applications of cumulants to array processing—part I: aperture extension and array calibration," *IEEE Transactions on Signal Processing*, vol. 43, no. 5, pp. 1200–1216, 1995.

[33] P. Chevalier and A. Férréol, "On the virtual array concept for the fourth-order direction finding problem," *IEEE Transactions on Signal Processing*, vol. 47, no. 9, pp. 2592–2595, 1999.


Journal of Engineering
The Scientific World Journal
International Journal of Rotating Machinery
Journal of Sensors
Advances in Multimedia
Advances in Civil Engineering
Journal of Control Science and Engineering
Journal of Robotics
Journal of Electrical and Computer Engineering
Advances in OptoElectronics
VLSI Design
International Journal of Navigation and Observation
Modelling & Simulation in Engineering
International Journal of Aerospace Engineering
International Journal of Chemical Engineering
International Journal of Antennas and Propagation
Active and Passive Electronic Components
Shock and Vibration
Advances in Acoustics and Vibration